Journal of Zhejiang University SCIENCE A
ISSN 1009-3095 (Print); ISSN 1862-1775 (Online)
www.zju.edu.cn/jzus; www.springerlink.com
E-mail: jzus@zju.edu.cn

Using FEM to predict tree motion in a wind field

Xiao-yi HU[†1,2], Wei-ming TAO[1], Yi-mu GUO[1]

([1]Department of Mechanical Engineering, Zhejiang University, Hangzhou 310027, China)

([2]School of Engineering, Zhejiang Forestry University, Hangzhou 311300, China)

[†]E-mail: jimhxy@zju.edu.cn

Received Oct. 21, 2007; revision accepted Jan. 28, 2008

Abstract: In this paper we propose a finite element (FE) simulation method to predict tree motion in a wind field. Two FE tree models were investigated: One model was generated based on a realistic nature-looking geometric tree model, and the other was a symmetric model to investigate the influence of asymmetric material properties on tree motion. The vortex-induced vibration (VIV) theory is introduced to estimate the fluctuating wind force being exerted on tree stems and the fluid-structure interaction (FSI) analysis is also included in the simulation. The results indicate that asymmetric material properties result in the crosswind displacement of the investigated node and the main swaying direction deviation. The simulation reveals that under wind loading, a tree with leaves has much larger swaying amplitude along the wind direction and longer swaying period than a tree without leaves. However, the crosswind swaying amplitude is mainly due to branch interaction. The numerical simulation proved that the interaction of tree branches can prevent dangerous swaying motion developing.

Key words: Finite element method (FEM), Fluid-structure interaction (FSI), Vortex-induced vibration (VIV), Asymmetric, Wind field

doi:10.1631/jzus.A0720035 **Document code:** A **CLC number:** O39; O368; S7

INTRODUCTION

The strongest influence on a tree's stability is wind force. And considerable research has been carried out to understand the mechanisms of wind-induced tree motions. Among all the research carried out, that conducted by Ken (2005) is very typical and he made some experiments to measure the tree motion in wind storms. His results indicated that trees are complex dynamic systems and trees sway in a complex looping manner under wind loading, but no explanation about the mechanism of the complex looping was given. Another important result of Ken (2005)'s research is that the branches of trees interact to prevent dangerous swaying motion developing, but no convincing numerical simulation had ever been conducted to prove this conclusion.

There have been many simplified numerical models of trees, but they were oversimplified and cannot explain the complex looping manner of a swaying tree. The oversimplified models included the harmonic oscillators (Gardiner, 1992; Baker, 1995; Ken, 2003) and the tapered cantilever beams (Saunderson *et al.*, 1999; Niklas, 2000; Ancelin *et al.*, 2004). These simplified models were all aimed at representing the swaying behavior of the main trunks of trees but they were all without branches and the interaction between tree branches was neglected.

Previous numerical models also oversimplified the mechanism of wind loading. In fact, the wind force exerted on a tree fluctuates due to vortex-shedding, and fluid-structure interaction (FSI) simulation is also necessary.

In this paper, two finite element (FE) tree models with branches are built and investigated. The dynamic simulation was carried out using the finite element method (FEM), which could provide a better way of explaining the mechanism of the complex looping manner of a swaying tree in a wind field and the interaction between tree branches. The theory of vortex-induced vibration (VIV) (Williamson and Govardhan, 2004) is introduced to estimate the fluctuating wind force exerted on tree stems and the FSI analysis is also included in the simulation.

FINITE ELEMENT MODEL

The FEM (Zienkiewicz and Taylor, 1991) is the most common numerical method used in solid mechanics to determine the stress and displacement fields in a domain in equilibrium.

Two FE tree models were investigated in this paper (Parameters of model-I and model-II are listed in Tables 1 and 2, respectively). The model-I (Fig.1) was generated based on a realistic nature-looking geometric tree model (Weber and Penn, 1995). The model-II (Fig.2) was a geometrically symmetric model for the special purpose of investigating the influence of asymmetric material properties on tree motion. Based on the assumption that at the site that the tree is located, the wind has a preferential direction, asymmetric material properties are formed because the tree reconfigures itself in response to wind forces by increasing the elastic modulus and density of the branches on the wind-exposed side.

Trunks and branches of trees were treated as tapered cantilever beams with a circular cross section and modeled in FE software using circular cross section beam elements. Preprocessing software MSC.-PATRAN was implemented in converting the geometry model into the FE model. A code based on PATRAN Command Language (PCL) was developed to achieve the fast conversion. Dynamic FE code MSC.Dytran was implemented to run the dynamic simulation.

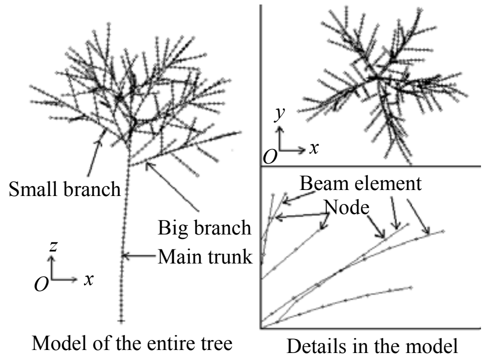

Fig.1 FE tree model-I (asymmetric model)

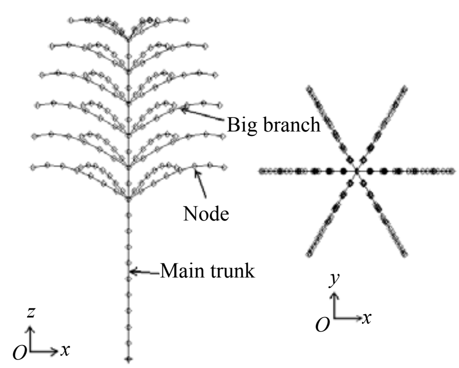

Fig.2 FE tree model-II (symmetric model)

Table 1 FE tree model-I

Parameter	Value	Reference
Total height (m)	18.0	Weber (1995)
Diameter at the bottom of the main trunk (m)	0.76	Weber (1995)
Diameter at the bottom of big branches (m)	0.06~0.25	Weber (1995)
Diameter at the bottom of small branches (m)	0.01~0.05	Weber (1995)
Density of the green wood (kg/m^3)	850	Wood Handbook (1999)
SME* of the main trunk (GPa)	10.0	Spatz *et al.*(2000)
SME* of big branches (GPa)	2.0~5.0	Hu *et al.*(2007)
SME* of small branches (GPa)	0.50	Hu *et al.*(2007)
Number of nodes	790	This paper
Material damping factor	0.05	Moore and Maguire (2004)
Natural frequency band and frequency peak of the tree system (obtained by x displacement spectrum) (Hz)	Frequency band: 0.22~0.53 (with leaves), 0.22~0.64 (without leaves); Frequency peak: 0.27, 0.38 (with leaves), 0.49, 0.27 (without leaves)	This paper

* SME: Structure modulus of elasticity

Table 2 FE tree model-II

Parameter	Value	Reference
Total height (m)	10.0	This paper
Diameter at the bottom of the main trunk (m)	0.40	This paper
Diameter at the bottom of big branches (m)	0.15	This paper
Density of the green wood (kg/m^3)	850	Wood Handbook (1999)
SME* of the main trunk (GPa)	10.0	Hu *et al.*(2007)
SME* of big branches (GPa)	2.0	Hu *et al.*(2007)
Number of nodes	143	This paper
Material damping factor	0.05	Moore and Maguire (2004)
Natural frequency band and frequency peak of the tree system (obtained by *x* displacement spectrum) (Hz)	Frequency band: 0.15~0.35 (with leaves) 0.15~0.43 (without leaves) Frequency peak: 0.17, 0.28 (with leaves) 0.34, 0.17 (without leaves)	This paper

* SME: Structure modulus of elasticity

An FE model is a space-discretized tree model, namely the tree is discretized into many nodes with concentrated masses and using beam elements to link them together. Through FE simulation, displacement at any node *i* can be achieved. A dynamic simulation is a time-discretized simulation, namely the time domain is divided into many small time steps. At time step *n*, the equation of motion that must be solved for the FE model of the tree is:

$$\boldsymbol{M}\boldsymbol{a}_n + \boldsymbol{C}\boldsymbol{v}_n + \boldsymbol{K}\boldsymbol{d}_n = \boldsymbol{F}_n^{\text{ext}}, \tag{1}$$

where $\boldsymbol{M}$ is the global mass matrix, which is of the order $3N$ ($3N$ is the degree of freedom of the discretized system), and N is the number of nodes of the FE tree model; $\boldsymbol{C}$ is the global damping matrix, which represents the material damping of the woody material of the tree; $\boldsymbol{K}$ is the global stiffness matrix; $\boldsymbol{a}_n$ is the global acceleration matrix at time step n; $\boldsymbol{v}_n$ is the global velocity matrix at time step n; $\boldsymbol{d}_n$ is the global displacement matrix at time step n; $\boldsymbol{F}_n^{\text{ext}}$ is the global vector of externally applied loads, namely the wind loads.

Eq.(1) can be written as:

$$\boldsymbol{a}_n = \boldsymbol{M}^{-1}\boldsymbol{F}_n^{\text{residual}}, \tag{2}$$

where $\boldsymbol{F}^{\text{residual}} = \boldsymbol{F}^{\text{ext}} - \boldsymbol{F}^{\text{int}}$ is the residual load vector, $\boldsymbol{F}_n^{\text{int}}$ is the vector of internal loads, $\boldsymbol{F}_n^{\text{int}} = \boldsymbol{C}\boldsymbol{v}_n + \boldsymbol{K}\boldsymbol{d}_n$.

For computational convenience, the assembled mass matrix M is lumped and presented in diagonal form. Since M is a diagonal matrix, its inversion is trivial, and the matrix equation is a set of independent equations for each degree of freedom, then acceleration can be derived by

$$a_{ni} = \boldsymbol{F}^{\text{residual}}/\boldsymbol{M}_i. \tag{3}$$

Assuming a constant acceleration during one time step, and using a central difference integration rule, velocity and displacement of all nodes can be obtained:

$$\boldsymbol{v}_{n+1/2} = \boldsymbol{v}_{n-1/2} + \boldsymbol{a}_n(\Delta t_{n+1/2} + \Delta t_{n-1/2})/2, \tag{4}$$

$$\boldsymbol{d}_{n+1} = \boldsymbol{d}_n + \boldsymbol{v}_{n+1/2}\Delta t_{n+1/2}. \tag{5}$$

WIND PROFILE

For natural wind the speed usually increases as the distance from the ground increases. In our simulation the wind speed $v_{\text{w}}(z)$ was considered as a function of the height above the ground. The wind profile was approximated according to the following logarithmic law:

$$v_w(z) = u_{TOP} \ln[1 + z(e-1)/H], \quad (6)$$

where u_{TOP} is the wind velocity at the highest point of the tree; H is the total height of the tree.

WIND FORCE CALCULATION

Two situations should be considered: A tree without a leaf and a tree full of leaves.

A tree without a leaf

For a tree without a leaf, the wind force acts directly on the tree branches. The branches of a tree can be regarded as circular cylinders. According to the theory of VIV, the vortex shedding will cause fluctuating drag and lift force on the tree branches. The vortex induced fluctuating force can be written as:

$$\boldsymbol{F}^{\text{ext}}(t) = \boldsymbol{F}_D(t) + \boldsymbol{F}_L(t), \quad (7)$$

where $\boldsymbol{F}_D(t)$ is the fluctuating drag force, which is along the wind direction; $\boldsymbol{F}_L(t)$ is the fluctuating lift force, which is vertical to the wind direction. The aerodynamic characteristics of a circular cylinder are significantly related to the Reynolds number, which is defined as

$$Re = (\rho v_w D)/u, \quad (8)$$

where ρ is air density, v_w is wind speed, D is diameter of the cylinder. A typical diameter of a tree stem is in the order of D=0.1 m, and in a general wind speed of 10 m/s, the corresponding Reynolds number is in the order of 10^4, which is within the sub-critical range. It is well known that at a sub-critical Reynolds number, the fluctuating pressures induced by vortex shedding on a circular cylinder yield periodic drag and lift forces.

Fig.3 is the fluctuating drag and lift coefficients derived by a wind tunnel study of a stationary circular cylinder with a diameter D=0.091 m and a length of 0.6 m (Nishimura and Taniike, 2001). The wind velocity was v_w=10 m/s giving the corresponding Reynolds number Re=6.1×10^4 which was in the above tree stem's Reynolds number range.

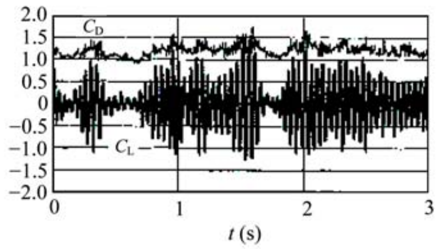

Fig.3 Drag (C_D) coefficient and lift coefficient (C_L) at Reynolds number 6.1×10^4 (Nishimura and Taniike, 2001)

The natural vortex shedding frequency f_0 of a stationary circular cylinder in the wind can be calculated by Eq.(9)

$$f_0 = (St \cdot v_w)/D, \quad (9)$$

where D is diameter of the circular cylinder; St is the Strouhal number, which is about 0.2 in Reynolds number range of 10^2~10^5.

The swaying frequency of a circular cylinder in flow is determined by the natural vortex shedding frequency f_0 and the natural oscillation frequency f_S of the structure. When f_0 is close to f_S, a cylinder subjected to flow induced vibrations exhibits the phenomenon of lock-in. The vortex shedding frequency related to the oscillating cylinder shifts to the frequency of cylinder vibrations. However, for a wind induced tree branch oscillation (with a regular wind speed, e.g., 10 m/s), f_0 is a hundred times larger than f_S and lock-in phenomenon will not happen. Thus, the tree branch oscillates at the natural vortex shedding frequency f_0.

Considering the beam element i on the tree model (Fig.4, and we can also find the elements i−1, i−2, etc.): this element can be regarded as having a

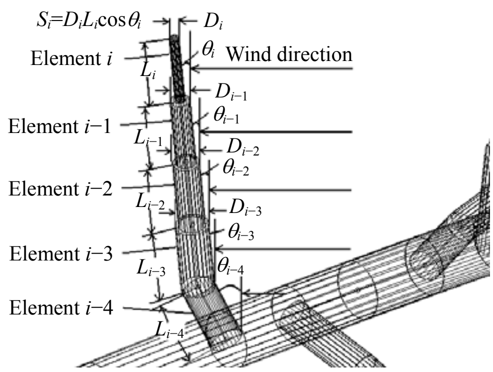

Fig.4 Wind force calculation

constant diameter D_i and length L_i. The fluctuating force on element i can be calculated by Eqs.(10)~(12):

$$f_i(t) = f_{Di}(t) + f_{Li}(t), \tag{10}$$

$$f_{Di}(t) = \frac{1}{2}\rho S_i C_D(t) v_w(t)^2, \tag{11}$$

$$f_{Li}(t) = \frac{1}{2}\rho S_i C_L(t) v_w(t)^2, \tag{12}$$

where $f_i(t)$ is the fluctuating force on element i due to wind, $f_{Di}(t)$ and $f_{Li}(t)$ are the fluctuating drag and lift forces on element i due to wind, respectively; ρ is the air density; S_i is the surface area of element i projected towards the wind (Fig.4).

$C_D(t)$ is the fluctuating drag coefficient, and in one vortex shedding period:

$$\int_t^{t+T_V} C_D(t)\mathrm{d}t = \overline{C}_D. \tag{13}$$

$C_L(t)$ is the fluctuating lift coefficient, and in one vortex shedding period:

$$\int_t^{t+T_V} C_L(t)\mathrm{d}t = 0. \tag{14}$$

According to Eqs.(10)~(14), the time-averaged force during time t_0 and time t_0+T_V in one vortex shedding period on element i can be written as:

$$\overline{f}_i\Big|_{t=t_0}^{t=t_0+T_V} = \frac{1}{2}\rho S_i \overline{C}_D v_w(t_0)^2. \tag{15}$$

A tree full of leaves

When a tree is full of leaves, most of the wind force is exerted on the leaves and the remainder on the branches. A tree leaf is very flexible and is bent severely by the wind, and this reduces the wind-exposed surface area and in turn reduces the wind force exerted on the leaf (Fig.5).

Fig.5 is the curve of the aerodynamic drag factor of a leaf bent in the wind, obtained by FSI simulation. The aerodynamic drag factor is supposed to be 1.0 at near zero wind speed; at a wind speed of 4 m/s, it drops to approximately 0.7; at a wind speed of 20 m/s, it drops to approximately 0.3. This dropping effect of the aerodynamic drag factor is considered during the simulation of a tree full of leaves.

Fig.6 is the FE model of the tree full of leaves and was generated by enclosing a virtual shell (coupling surface) on the canopy of the FE tree model-I. The wind force is supposed to be fully exerted on the tree canopy surface and then passes to the tree. The canopy surface was combined with a virtual shell and set to be the coupling surface. During the simulation, the aerodynamic drag factor was dropping as the wind speed was increasing with respect to the drag factor curve in Fig.5.

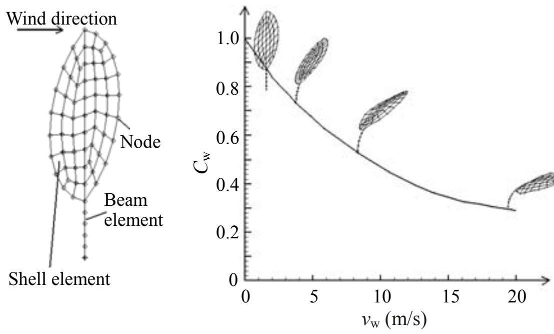

Fig.5 FE simulation result of a leaf in wind field

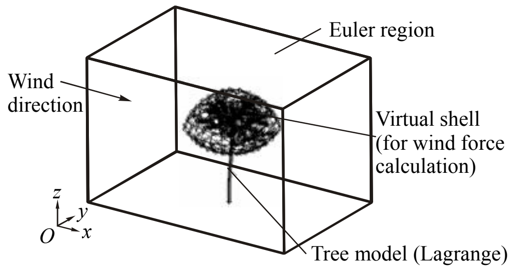

Fig.6 FSI analysis of the FE tree model-I with leaves

FSI analysis is carried out in the simulation. The wind region was meshed using Euler mesh, the tree and the virtual shell were meshed using a Lagrange mesh. The virtual shell was the coupling surface in the simulation and the wind force exerted on the virtual shell was automatically calculated by the FE code MSC.Dytran and at the same time exerted on the tree as an external load.

From the above discussion it can be noted that the fluctuating wind force exerted on tree branches was calculated using the formulation for stationary circular cylinders. However, tree branches move in the wind. Is it feasible to use the formulation and experimental data for a stationary cylinder for estimating the wind force on moving tree branches? The answer is "yes". Compared with a leaf, a branch is much heavier and this means that an investigation point on a branch will have a much longer oscillation period than that on a leaf. Furthermore, the oscillation period of a branch is much longer than that of vortex shedding. In one vortex shedding period the displacement of a tree branch is small and will not significantly influence the wind force exerted on the branch. The error induced by the simplification is small compared with the errors caused by other factors, such as the errors of branch diameter measurements, the errors of material property measurements, etc.

RESULTS AND DISCUSSION

Fig.7a is a 10 s sample of motion for the investigated node of the FE tree model-I, which is obtained by exerting the time-averaged wind load on the FE tree model-I. The investigated node on the tree moves in a complex looping manner. Without considering no wind force in a crosswind direction was exerted on the influence of vortex shedding, the tree but crosswind displacement occurs, due to the interaction of tree branches.

Fig.7b is a 10 s sample of motion of the investigated node taking into consideration the influence of vortex shedding. This sample of motion is obtained by exerting the vortex induced fluctuating wind load on the FE tree model-I. The vortex-induced fluctuation of the motion track can be clearly seen. However, the amplitude of vortex-induced fluctuation is magnified one hundred times because it is actually very small. Without magnifying the vortex-induced fluctuation, the fluctuation in Fig.8 is not visible.

Fig.8a is a 10 s sample of motion for the investigated node of the FE tree model-II with fully symmetric material properties. The nodal displacement of the investigated node coincides with the wind direction and no displacement of crosswind direction is observed.

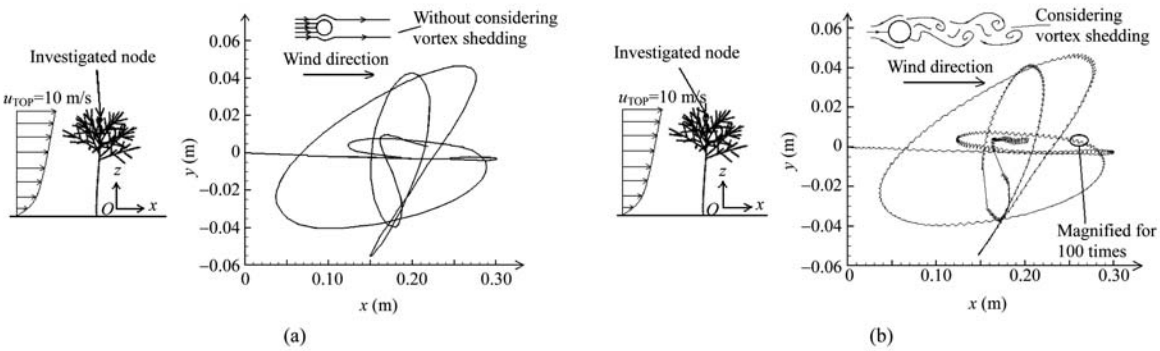

Fig.7 Sample of motion for the investigated node of the FE tree model-I. (a) Without vortex shedding; (b) With vortex shedding

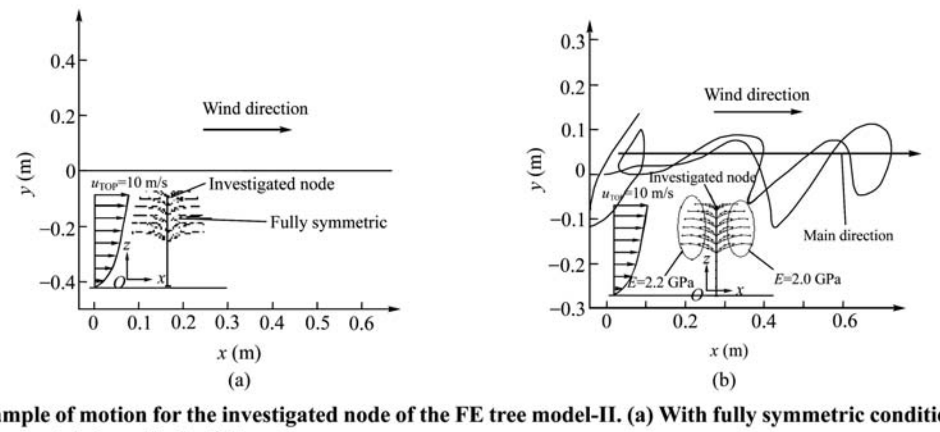

Fig.8 Sample of motion for the investigated node of the FE tree model-II. (a) With fully symmetric condition; (b) With asymmetric branch elasticity

Fig.8b is a 10 s sample of motion for the investigated node of the FE tree model-II with asymmetric branch elasticity. The elastic modulus on the wind-exposed side of the tree branches is 10% larger than that on the leeward side. The main direction of the nodal displacement is still coinciding with the wind direction. However, the crosswind displacement occurs and the motion track is in a looping shape.

Fig.9 is a 10 s sample of motion for the investigated node of FE tree model-II with asymmetric branch density. The density of the wind-exposed side of the tree branches is 10% larger than that of the leeward side. The main direction of the node displacement is deviating from the wind direction and the motion track is in a looping shape.

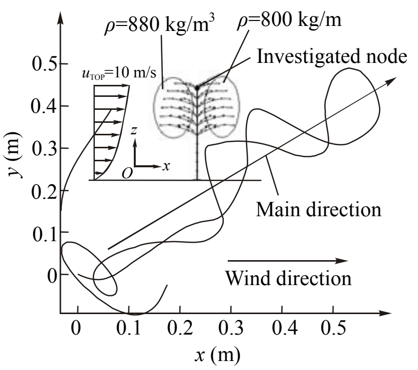

Fig.9 Sample of motion for asymmetric branch density (model-II)

Figs.10a and 10b show the comparison between the displacement of the investigated nodes of the trees with and without leaves based on the FE tree model-I. Fig.10a indicates that along the wind direction (x) the tree with leaves has a much larger displacement and longer swaying period than the tree without leaves. However, Fig.10b indicates that along the crosswind direction (y), the tree with leaves does not have a much larger displacement than the tree without leaves, and that the swaying period also shows smaller differences. It can be concluded that the crosswind displacement is mainly due to the branch interaction but does not has much relation to leaves. Leaves will significantly increase the wind force exerted on a tree, but mainly along the wind direction.

Fig.11 is the comparison of the x displacement of the investigated node of the tree with the FE tree model-I and a cantilever beam model. When the wind excitation frequency coincides with the natural swaying frequency (Baker, 1997; Moore and Maguire, 2004) of the cantilever beam model, the resonance is observed and the amplitude increases with time. However, for a tree with branches (our model), the resonance will not be observed even when the wind excitation frequency coincides with the natural swaying frequency of the tree. This simulation result proved that the interaction of tree branches can prevent a dangerous swaying motion developing.

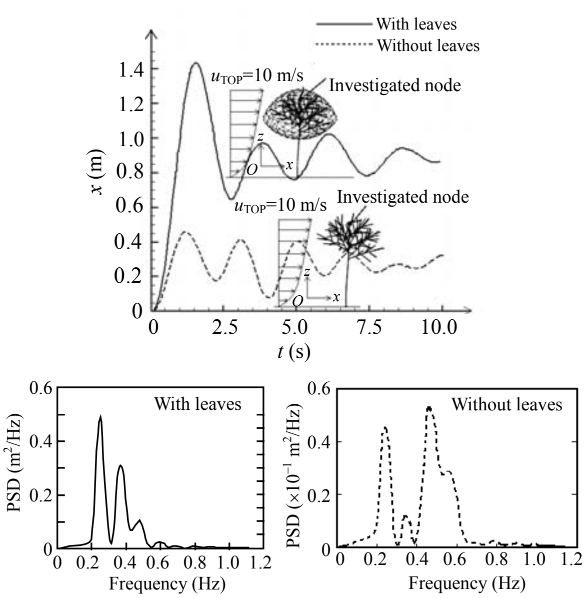

(a)

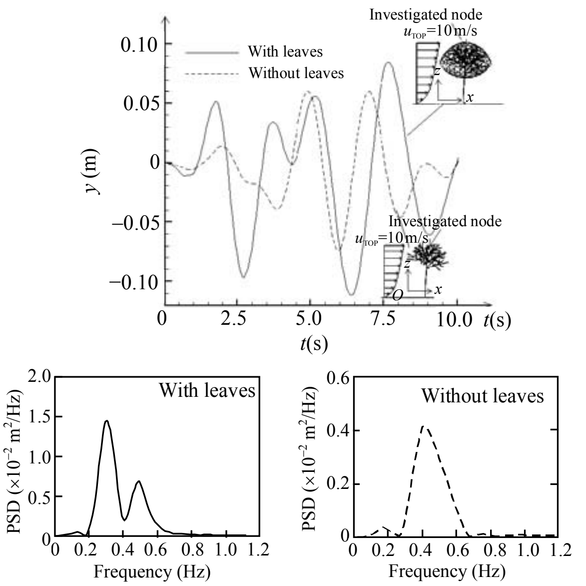

(b)

Fig.10 Comparison of x displacement (a) and y displacement (b) With and without leaves (model-I)

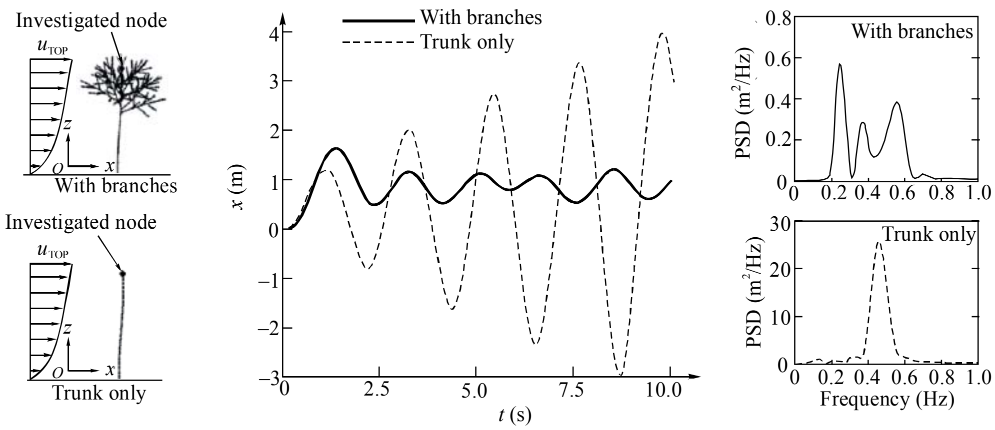

Fig.11 Tree with branches and trunk only in fluctuating wind (model-I)

In order to get lucid information on the period of oscillation of a tree in different conditions in Figs.10~11, Fourier power spectrum of the oscillating signal was made and presented in the figures. The information concerning displacement spectra in Figs.10a and 10b revealed that the tree with leaves has a lower frequency peak for both x and y displacements, and the frequency is about 0.27 Hz. For the tree without leaves, the lower frequency is not dominant. This is especially true for the y displacement (Fig.10b, the lower frequency peak is very low and has nearly disappeared). It can be explained that the lower frequency peaks are mainly due to the effect of the leaves. For both the trees with and without leaves, higher frequency peaks also exist. Differing from the lower frequency, which is almost identical (equal to 0.27 Hz) in both circumstances, the higher frequency differs under different circumstances: 0.38 Hz for the tree with leaves and x displacement, 0.49 Hz for the tree without leaves and x displacement, 0.50 Hz for the tree with leaves and y displacement, 0.45 Hz for the tree without leaves and y displacement. The higher frequency may mainly be determined by the natural swaying frequency of the oscillation system including the main trunk and big branches; the frequency difference under different circumstances may be caused by the asymmetric geometric property of the tree model. The information about displacement spectrum in Fig.11 is very easy to interpret, namely that the spectrum for the isolated trunk has a much higher peak and a narrower frequency band than the spectrum for the tree with branches. From a physics point of view, the isolated trunk is like a cantilever beam fixed at one end, it definitely has just one frequency peak in its spectrum, and due to the resonate oscillation the peak will be very high. On the other hand, the frequency band is wide for the tree with branches. This is due to the interaction between branches, and which can prevent resonate oscillation developing. The spectrum in Fig.11 for the tree with branches also differs from those in Figs.10a and 10b, due to different wind loading condition. Fluctuating wind loading definitely causes a different oscillation from a constant wind loading.

DISACUSSION AND CONCLUSION

In this paper, we present an FE simulation method to predict tree motion under wind loading. When compared with those models describing a tree as having harmonic oscillators or a single cantilever beam, the FE tree model has branches and this enrichment enables the simulation of a complex interaction of tree branches.

To adapt the external wind load, the tree always reconfigures itself by increasing the elastic modulus and density of the branch material on the wind-exposed side. Subsequently, asymmetric material properties of tree branches will result in a complex looping movement of the tree under wind loading. This is an explanation of the mechanism of Ken (2005)'s experimental discovery for the complex looping movement of a tree under wind loading.

Under wind loading, leaves significantly increase the wind force exerted on a tree and subsequently increase the swaying amplitude along the wind direction. However, the crosswind swaying amplitude of a tree is mainly due to branch interaction and is little affected by the leaves. Spectrum analysis revealed that the tree with leaves has a lower frequency peak and the frequency is about 0.27 Hz. It can be explained that the lower frequency peak is mainly due to the influence of the leaves. The higher frequency peak on the other hand may mainly be due to the main trunk and big branches.

Finally, the simulation result of the FE tree model also proved that the interaction of tree branches can prevent dangerous swaying motion developing.

References

Ancelin, P., Courbaud, B., Thierry, F., 2004. Development of an individual tree-based mechanical model to predict wind damage within forest stands. *Forest Ecology and Management*, **203**(1-3):101-121. [doi:10.1016/j.foreco.2004.07.067]

Baker, C.J., 1995. The development of a theoretical model for the windthrow of plants. *Journal of Theoretical Biology*, **175**(3):355-372. [doi:10.1006/jtbi.1995.0147]

Baker, C.J., 1997. Measurements of the natural frequencies of trees. *Journal of Experimental Botany*, **48**(5):1125-1132. [doi:10.1093/jxb/48.5.1125]

Gardiner, B.A., 1992. Mathematical Modeling of the Static and Dynamic Characteristics of Plantation Trees. *In*: Franke, J., Roeder, A. (Eds.), Mathematical Modeling of Forest Ecosystems. Sauerlander, Frankfurt/Main, p.40-61.

Ken, J., 2003. Dynamic loading of trees. *Journal of Arboriculture*, **29**(3):165-171.

Ken, J., 2005. Dynamic Wind Loads on Trees. Tree Dynamics, Isaac, http://isaac.org.au/files/wott/Dynamic%20Wind%20Loads%20on%20trees.pdf, downloaded in July, 2006.

Moore, J.R, Maguire, D.A., 2004. Natural sway frequencies and damping ratios of trees: concepts, review and synthesis of previous studies. *Trees*, **18**:195-203.

Niklas, K.J., 2000. Computing factors of safety against wind-induced tree stem damage. *Journal of Experimental Botany*, **51**(345):797-806. [doi:10.1093/jexbot/51.345.797]

Nishimura, H., Taniike, Y., 2001. Aerodynamic characteristics of fluctuating forces on a circular cylinder. *Journal of Wind Engineering and Industrial Aerodynamics*, **89**:713-723.

Saunderson, S.E.T., England, A.H., Baker, C.J., 1999. A dynamic model of the behaviour of sitka spruce in high winds. *Journal of Theoretical Biology*, **200**(3):249-259. [doi:10.1006/jtbi.1999.0983]

Weber, J., Penn, J., 1995. Creation and Rendering of Realistic Trees. Proceedings of the SIGGRAPH'95 Annual Conference. ACM Press, New York, p.119-127.

Williamson, C.H.K., Govardhan, R., 2004. Vortex-induced vibrations. *Annual Review of Fluid Mechanics*, **36**(1):413-455. [doi:10.1146/annurev.fluid.36.050802.122128]

Wood Handbook, 1999. Wood as an Engineering Material. USDA Forest Products Laboratory, Madison, Wisconsin.

Zienkiewicz, O.C., Taylor, R.L., 1991. The Finite Element Method. McGraw-Hill, New York.